INFECTIOUS DISEASE

Zika virus activates de novo and cross-reactive memory B cell responses in dengue-experienced donors

Thomas F. Rogers,[1]* Eileen C. Goodwin,[2]* Bryan Briney,[1] Devin Sok,[1] Nathan Beutler,[1] Alexander Strubel,[1] Rebecca Nedellec,[1] Khoa Le,[1] Michael E. Brown,[2] Dennis R. Burton,[1,3]† Laura M. Walker[2]†

Zika virus (ZIKV) shares a high degree of homology with dengue virus (DENV), suggesting that preexisting immunity to DENV could affect immune responses to ZIKV. We have tracked the evolution of ZIKV-induced B cell responses in three DENV-experienced donors. The acute antibody (plasmablast) responses were characterized by relatively high somatic hypermutation and a bias toward DENV binding and neutralization, implying the early activation of DENV clones. A DENV-naïve donor in contrast showed a classical primary plasmablast response. Five months after infection, the DENV-experienced donors developed potent type-specific ZIKV neutralizing antibody responses in addition to DENV cross-reactive responses. Because cross-reactive responses were poorly neutralizing and associated with enhanced ZIKV infection in vitro, preexisting DENV immunity could negatively affect protective antibody responses to ZIKV. The observed effects are epitope-dependent, suggesting that a ZIKV vaccine should be carefully designed for DENV-seropositive populations.

INTRODUCTION

Zika virus (ZIKV) is a mosquito-borne flavivirus that has been linked to microcephaly and severe neurological complications, such as Guillain-Barré syndrome (*1*, *2*). The virus is closely related to the four serotypes of dengue virus (DENV) (DENV1, 2, 3, and 4), as well as other circulating flaviviruses including West Nile virus (WNV), resulting in substantial immunological cross-reactivity (*3*–*7*). Although neutralizing antibodies (nAbs) play an important role in protection against flavivirus infection, they can also contribute to severe disease through a phenomenon termed antibody-dependent enhancement (ADE) (*8*–*10*). In the case of DENV, subneutralizing concentrations of preexisting heterotypic nAbs have been implicated in promoting viral replication by facilitating the interaction of the virus with Fc receptor–bearing target cells (*8*). Enhancement of ZIKV infection by cross-reactive DENV-specific antibodies and vice versa has been demonstrated in vitro, and ADE of ZIKV pathogenesis by preexisting anti-flavivirus immunity has been observed in mouse models (*5*–*7*, *11*–*14*). Because ZIKV is currently circulating in regions that are highly endemic for DENV, an understanding of how previous DENV exposure affects the B cell response to ZIKV will be critical for the design of vaccines and therapies intended for DENV-immune populations.

Previous studies have shown that nonstructural protein 1 (NS1), envelope (E), and precursor membrane (prM) proteins are dominant targets for the human B cell response to flaviviruses. NS1 is secreted by infected cells and functions in pathogenesis and immune evasion (*15*), the surface E protein mediates viral entry and is the primary target for nAbs (*7*, *16*, *17*), and prM is a 166–amino acid protein that is associated with E on immature and partially mature viruses (*18*). The E protein consists of three domains: domain I (DI), which participates in conformational changes required for viral entry; domain II (DII), which contains the conserved fusion loop (FL); and domain III (DIII), which is the putative receptor binding domain (*19*). Previous studies have established that monoclonal antibodies (mAbs) targeting epitopes within DIII are typically type-specific and potently neutralizing, whereas mAbs targeting the conserved FL are cross-reactive and poorly neutralizing (*7*, *16*, *17*, *20*).

In this study, we have longitudinally tracked the ZIKV-specific B cell response in three DENV-experienced donors using single B cell cloning and large-scale antibody isolation. The acute-phase (plasmablast) response was dominated by somatically mutated clones that showed preferential binding and neutralization of DENV, providing evidence for original antigenic sin (OAS) during the early B cell response to ZIKV in DENV-experienced donors. However, by 5 months after infection, the memory B cell responses were composed of both OAS-phenotype antibodies that were broadly cross-reactive and poorly neutralizing and de novo generated antibodies that were ZIKV-specific and potently neutralizing. Collectively, the results have implications for the development of ZIKV vaccines intended for DENV-immune populations and provide insight into the role that preexisting B cell memory plays in modulating the antibody specificities induced by antigenically variable viruses.

RESULTS

Potent plasmablast induction in ZIKV-infected, DENV-experienced donors

To study the early ZIKV-induced B cell response in DENV-experienced individuals, three ZIKV-infected donors (donors 2, 3, and 4) living in a highly DENV endemic region of Colombia were sampled during acute infection (within 8 days after symptom onset) (table S1) (*21*). A single donor (donor 1) from the United States who was infected with ZIKV while overseas was also sampled for comparison (table S1). As expected, the acute sera from donors 2, 3, and 4 showed strong immunoglobulin G (IgG) binding reactivity to whole DENV1–4 particles and recombinant DENV NS1 proteins (fig. S1). In contrast, the acute serum from donor 1 showed little to no such binding (fig. S1). Although the acute serum reactivity to DENV particles and NS1 proteins could, in principle, be due to cross-reactive ZIKV-induced antibodies, previous studies have shown that NS1-specific IgG antibodies are not present in the serum during the first week

[1]Department of Immunology and Microbiology, the Scripps Research Institute, La Jolla, CA 92037, USA. [2]Adimab LLC, Lebanon, NH 03766, USA. [3]Ragon Institute of MGH, MIT and Harvard, Cambridge, MA 02139, USA.
*These authors contributed equally to this work.
†Corresponding author. Email: laura.walker@adimab.com (L.M.W.); burton@scripps.edu (D.R.B.)

after the onset of symptoms of ZIKV infection (*22*, *23*), implying that the acute serum reactivity to DENV NS1 observed for donors 2, 3, and 4 is largely mediated by preexisting antibodies that were induced by previous DENV exposure. Furthermore, the acute serum from these three donors showed similar or more potent neutralizing activity against DENV compared with ZIKV, whereas the acute serum from donor 1 showed little to no neutralizing activity against DENV1–4 and relatively weak neutralization of ZIKV. These serological and epidemiological data provide convincing evidence that donors 2, 3, and 4 were previously exposed to DENV, whereas donor 1 was DENV-naïve at the time of infection.

The appearance of antigen-specific plasmablasts in peripheral blood during acute viral infection is typically the first indication of a B cell response (*24*–*26*). Therefore, we first measured the plasmablast frequency in peripheral blood about 1 week after symptom onset (table S1). In all three DENV-experienced donors, a massive plasmablast population ($CD3^-CD20^{-/lo}CD19^+CD27^{hi}CD38^{hi}$) that accounted for 39 to 63% of peripheral B cells was observed (Fig. 1A and fig. S2). In contrast, the plasmablast population in the ZIKV-infected, DENV-naïve donor was relatively small, accounting for only 2.5% of peripheral B cells (Fig. 1A). To deconstruct the acute ZIKV-induced B cell response, we single cell–sorted between 100 and 300 plasmablasts from each donor sample and rescued the antibody variable heavy (V_H) and variable light (V_L) chain sequences by single-cell polymerase chain reaction (PCR). Between 42 and 119 cognate V_H and V_L pairs from each donor were cloned and expressed as full-length IgGs. Sequence analysis revealed that the plasmablasts sorted from the three DENV-experienced donors were somatically mutated—with per-donor averages ranging between 15 and 20 nucleotide substitutions in V_H—and clonally expanded (Fig. 1, B and C). This level of somatic hypermutation (SHM) is comparable with that observed in typical IgG^+ memory B cells as well as in plasmablasts induced by influenza vaccination (*25*), supporting a memory B cell origin for these acutely induced cells. In contrast, most of the plasmablasts isolated from the DENV-naïve donor sample showed little to no SHM and somewhat more limited clonal expansion (Fig. 1, B and C), supporting their emergence via activation of naïve B cells. We conclude that ZIKV infection induces a rapid and robust plasmablast response in DENV-experienced donors and that the large majority of these acutely induced cells appear to originate from the memory B cell compartment.

A large proportion of plasmablast-derived mAbs isolated from ZIKV-infected, DENV-experienced donors bind the ZIKV E protein

Enzyme-linked immunosorbent assay (ELISA) binding studies showed that between 50 and 75% of the mAbs isolated from the DENV-experienced donors bound to whole ZIKV (fig. S3), which is similar to the percentage of antigen-specific mAbs recovered from plasmablasts induced by influenza vaccination and DENV infection (*25*, *27*). In contrast, only 13% of the plasmablast-derived mAbs isolated from the DENV-naïve donor bound with detectable affinity to whole ZIKV particles. To further map the antigenic specificities of the 303 plasmablast-derived mAbs, we performed biolayer interferometry (BLI) binding experiments with recombinant ZIKV NS1 and E proteins. The percentage of mAbs isolated from the three DENV-experienced donors that showed reactivity with ZIKV NS1 was low at 8 to 12% and higher for recombinant E at 15 to 39% (Fig. 2A and table S2). In contrast, 17% of the mAbs isolated from the DENV-naïve donor bound to recombinant NS1, whereas only a single mAb bound with detectable affinity to recombinant E (Fig. 2A and table S2). The remaining ZIKV-specific mAbs, which accounted for 13 to 32% of the corresponding donor responses, bound to epitopes expressed on whole virus but not on recombinant E. Seventy percent of the plasmablast mAbs isolated from donor 1 and about 20 to 50% of the

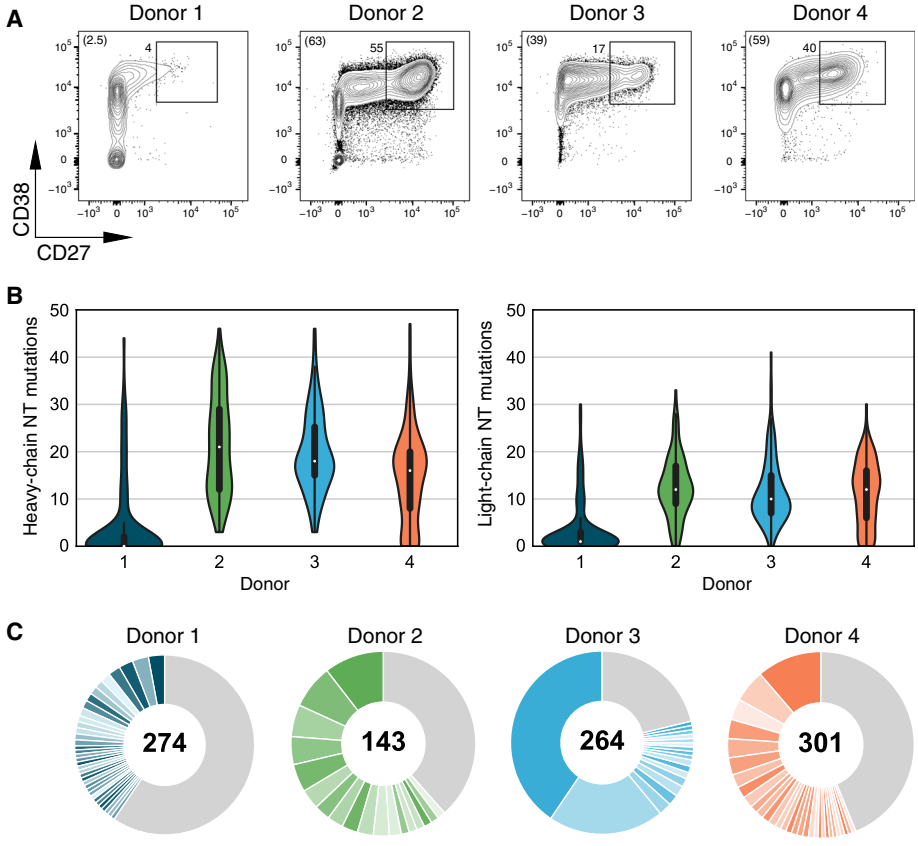

Fig. 1. Analysis of plasmablast responses in one naïve and three DENV-experienced donors. (**A**) Flow cytometric analysis of plasmablast responses in one naïve and three DENV-experienced donors during ongoing ZIKV infection. Plasmablasts are defined herein as $CD19^+CD3^-CD20^{-/lo}CD38^{hi}CD27^{hi}$ cells. Plots shown are gated for $CD3^-CD20^{-/lo}$ cells, with the $CD27^{hi}CD38^{hi}$ plasmablasts marked by a box. The frequency of plasmablasts within the $CD3^-CD20^{-/lo}$ population is shown next to the gate. The numbers in parentheses show the percentage of peripheral B cells that are plasmablasts. Flow cytometry data were analyzed using FlowJo software (version 10.0.8). (**B**) Load of somatic mutations [expressed as the number of nucleotide (NT) substitutions] in V_H and V_L in plasmablast-derived mAbs isolated from a DENV-naïve (donor 1) and three DENV-experienced donors (donors 2 to 4). All V_H and V_L chains are shown, regardless of whether the paired antibody chain was recovered. (**C**) Clonal lineage analysis. Heavy-chain sequences were assigned to lineages using Clonify (*52*). Each lineage is represented as a segment proportional to the lineage size. The total number of recovered heavy chains is shown in the center of each pie. All lineages that contain only a single sequence are combined and shown as a single gray segment.

plasmablast mAbs isolated from donors 2, 3, and 4 could not be associated with any ZIKV reactivity (Fig. 2A). Because anti-prM antibodies have been shown to dominate the antibody response during secondary DENV infection (*28*), we next investigated the specificities of the whole virus–specific mAbs isolated from the DENV-experienced donors by Western blot. None of the mAbs recognized prM, 30% showed reactivity with E protein from viral lysates, and the remaining mAbs failed to bind to ZIKV in this assay (fig. S4). Hence, most of these mAbs likely bind to E-specific epitopes expressed only on intact virions. Similar specificities have been previously described for both DENV and ZIKV (*4*, *7*, *27*, *29*).

To further define the epitopes targeted by the recombinant E–reactive mAbs isolated from the DENV-experienced donors, we (i) compared the apparent binding affinities of the mAbs for recombinant

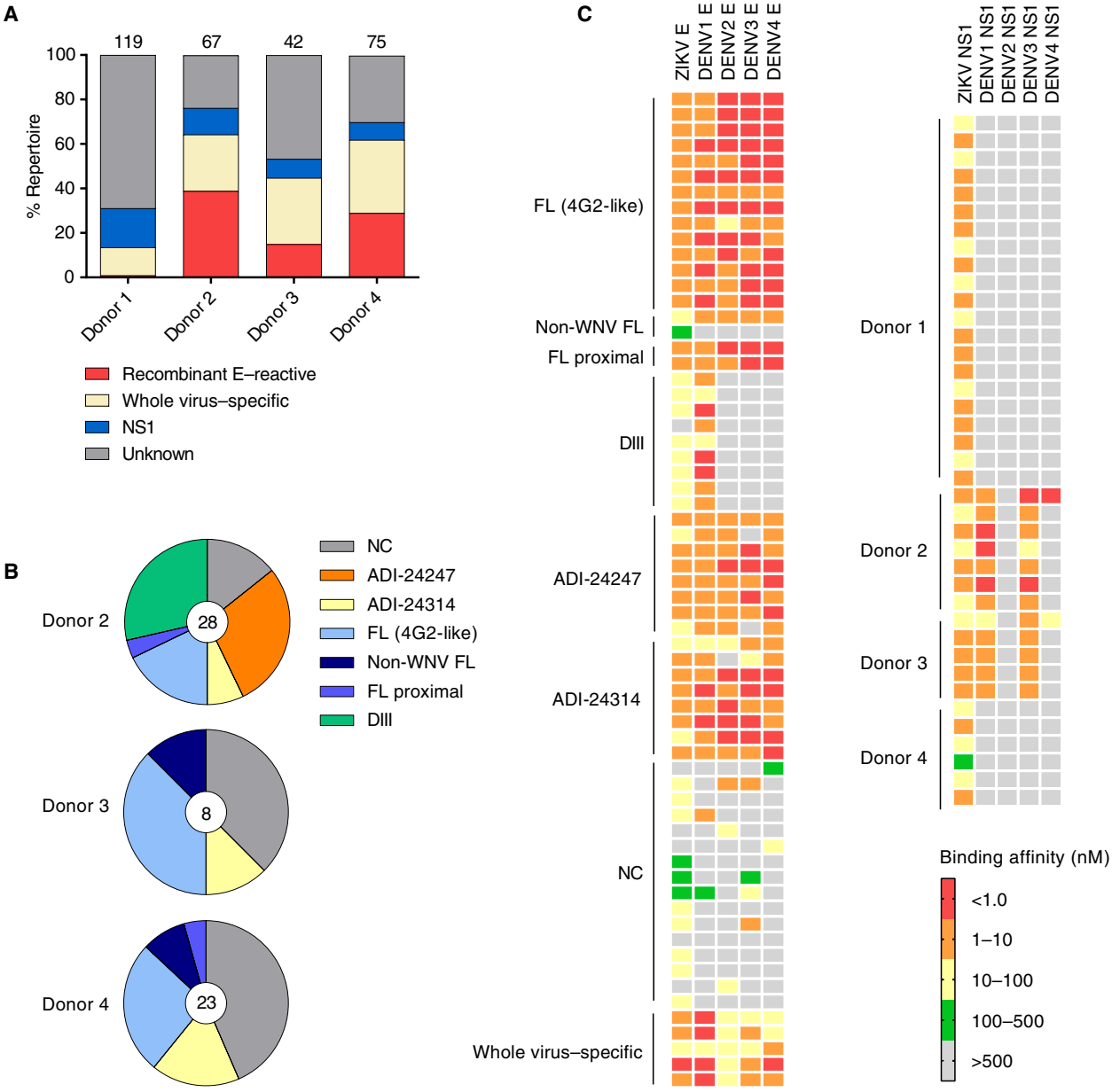

Fig. 2. Binding characteristics of mAbs isolated from plasmablasts during acute ZIKV infection. (**A**) Specificities of the mAbs isolated from one DENV naïve donor and three DENV-experienced donors. Distribution of mAbs that bind to NS1, recombinant E, epitopes expressed only on whole ZIKV, and those for which no specificity could be assigned are shown. The number at the top of each bar represents the total number of mAbs cloned from each donor. (**B**) Epitope mapping of recombinant E–specific antibodies isolated from three DENV-experienced donors. Pie charts show the distribution of antibodies that bind to epitopes within DIII, within or proximal to the FL on DII, and defined by mAbs ADI-24314 and ADI-24247. 4G2-like FL: Competition with 4G2, WNV E–reactive, and E-FL–sensitive; non-WNV FL: 4G2-competitive, E-FL–sensitive, and WNV E–nonreactive; FL proximal: 4G2 competitive, E-FL–reactive, and WNV E–nonreactive; DIII: Recombinant DIII–reactive; ADI-24314 competitor: 4G2-noncompetitive, ADI-24314–competitive, and E-FL–reactive; ADI-24247 competitor: 4G2-noncompetitive, ADI-24247–competitive, and E-FL–reactive. NC, not characterized because of low binding affinity. (**C**) Heat map of mAb binding reactivity to ZIKV and DENV1–4 E proteins or whole viral particles (left) and ZIKV and DENV1–4 NS1 proteins (right). The E-specific mAbs shown were isolated from DENV-experienced donors. Apparent binding affinities for recombinant E and NS1 proteins were determined by BLI measurements, and apparent binding affinities for whole virus were determined by ELISA.

DIII, WNV E, and a previously described ZIKV E protein (E-FL) that contains substitutions within and proximal to the FL that abolish binding by most FL-specific antibodies (*30*) (fig. S5) and (ii) performed competitive binding experiments using two previously characterized mAbs, 4G2 and ZV-67, that bind to the FL on DII and the lateral ridge on DIII, respectively (table S2) (*30*, *31*). Because the FL-specific mAb 4G2 reacts with WNV E and fails to react with E-FL (table S3), we classified mAbs that competed with 4G2, bound to WNV E, and failed to bind to E-FL as "4G2-like FL binders." 4G2 competitor mAbs that failed to bind to E-FL but did not cross-react with WNV E were classified as "non-WNV FL binders," and 4G2 competitor mAbs that did not cross-react with WNV E but did bind to E-FL were classified as "FL proximal binders." Together, mAbs that bound within or proximal to the FL comprised up to 50% of the recombinant E–reactive responses (Fig. 2B and table S2). DIII-specific mAbs were absent from the donor 3 and donor 4 responses but comprised about 30% of the donor 2 response (Fig. 2B and table S2). Six of eight DIII-reactive mAbs competed with ZV-67, suggesting that they likely recognize epitopes within or proximal to the lateral ridge on DIII (table S2). This class of antibodies showed preferential VH3-23 germline gene usage and contained convergent sequence signatures in both CDRH3 and CDRL3 (table S4), suggesting that these mAbs may share a common mode of antigen recognition. To estimate the number of different antigenic sites recognized by the remaining E-specific mAbs, we performed competitive binding experiments with two broadly cross-reactive mAbs from the panel (ADI-24247 and ADI-24314) that did not compete with 4G2, ZV-67, or each other (tables S2 and S5). Between 12 and 35% of the E-specific donor responses bound to epitopes overlapping that of ADI-24247 or ADI-24314 (Fig. 2B). Overall, we conclude that substantial fractions of the acute ZIKV-induced B cell response in DENV-experienced donors are directed against quaternary epitopes expressed only on whole virus, and those that are reactive with recombinant E are largely directed to the FL and other highly conserved epitopes.

The ZIKV-induced plasmablast response in DENV-experienced donors is dominated by DENV cross-reactive clones

The E proteins of ZIKV and DENV share more than 50% sequence identity, resulting in substantial immunological cross-reactivity (*3*, *6*, *7*). To determine the degree to which mAbs generated from plasmablasts during acute ZIKV infection cross-reacted with DENV, we measured the apparent binding affinities of the mAbs for recombinant DENV1–4 E and NS1 proteins. Most of the E-specific mAbs from the three DENV-experienced donors bound with higher affinity to at least one of the four DENV E proteins than to ZIKV E, consistent with a recall response dominated by reactivated DENV-induced memory B cells (Fig. 2C, table S2, and fig. S6). Selected mAbs isolated from donors 2, 3, and 4 that targeted epitopes expressed only on whole ZIKV showed similar DENV-biased binding profiles (fig. S7). In contrast, the whole virus–specific mAbs isolated from donor 1 bound exclusively to ZIKV (fig. S7).

About 50% of the ZIKV E–reactive mAbs isolated from the DENV-experienced donors cross-reacted with all four DENV serotypes (Fig. 2C and table S2). Most of these broadly cross-reactive mAbs targeted epitopes within or proximal to the FL or unknown epitopes defined by ADI-24247 and ADI-24314 (Fig. 2C and table S2). In contrast, the DIII-specific mAbs only showed cross-reactivity with DENV1 E (Fig. 2C and table S2). One hundred percent of the NS1-specific mAbs isolated from donors 2 and 3 showed cross-reactivity with DENV1 and DENV3 NS1, whereas the NS1-specific mAbs from donor 4 were exclusively ZIKV-specific (Fig. 2C and table S6). Sequence analysis revealed that the ZIKV NS1-specific mAbs from donor 4 lacked SHM, supporting a naïve B cell origin (fig. S8). The reasons for this are unclear but may be due to the lack of preexisting cross-reactive NS1-specific memory B cells in this donor. As expected, all of the NS1-specific mAbs isolated from donor 1 were ZIKV-specific and lacked SHM (Fig. 2C). The affinities of these mAbs were comparable with the affinities of the NS1-specific mAbs isolated from the DENV-experienced donors (Fig. 2C and table S6), which is perhaps because the plasmablast-derived antibodies from the DENV-experienced donors had not undergone affinity maturation toward ZIKV. Together, the sequencing and binding results provide evidence for OAS during the acute-phase B cell response to ZIKV in DENV-experienced donors.

Most of the plasmablast-derived mAbs isolated from DENV-experienced donors are poorly neutralizing and potently enhancing

To assess the functional properties of the plasmablast-derived mAbs isolated from the DENV-experienced donors, we next performed neutralization and ADE assays. Because of the large number of mAbs, initial neutralization screening was performed using a single concentration of purified IgG. At a concentration of 1 μg/ml, about 20% of mAbs from each donor reduced ZIKV-Paraiba (Para) infectivity by ≥50%, and all of these nAbs cross-neutralized at least one of the four DENV serotypes (Fig. 3A). Additionally, the majority of nAbs (53 of 63 or 84%) showed more potent neutralizing activity against one of the four DENV serotypes than ZIKV-Para (Fig. 3A). We next performed neutralization titration experiments on a subset of mAbs to evaluate neutralization potency. Consistent with the binding and single-point neutralization results, a large proportion of mAbs showed preferential neutralization of DENV, further supporting a DENV-induced memory B cell origin for these recently activated cells (Fig. 3B, table S7, and fig. S9). Of significance, most of the plasmablast-derived mAbs showed poorly neutralizing activity against ZIKV-Para (Fig. 3, B and C). The notable exceptions were the four DIII-specific mAbs, which showed highly potent neutralizing activity against both ZIKV-Para and DENV1 (Fig. 3, B and C, and table S7). These nAbs displayed IC_{50}s (half-maximal inhibitory concentrations) between 0.9 and 2.7 ng/ml against ZIKV-Para and between 0.2 and 27 ng/ml against DENV1 (Fig. 3, B and C, and table S7). Most of the mAbs that bound to quaternary epitopes on the E protein showed little to no neutralizing activity against ZIKV. Previous studies have described two classes of quaternary mAbs (EDE1 and EDE2), which are defined on the basis of differing sensitivity to removal of the N-glycan at Asp^{153} (*4*). Given that mAbs directed against EDE2 have been shown to be substantially less potent against ZIKV than mAbs targeting EDE1, it is likely that the quaternary mAbs described here recognize the EDE2 epitope.

We next tested the abilities of selected mAbs to enhance ZIKV infection using nonpermissive K562 cells. Consistent with previous studies, all of the mAbs enhanced ZIKV infection, but peak enhancement was observed at lower concentrations for the potently neutralizing DIII-specific mAbs compared with the poorly neutralizing cross-reactive mAbs (fig. S10) (*6*, *7*, *16*, *32*). Additionally, there was a linear correlation between neutralization potency and the sum of the enhancement activity over the range of mAb concentrations tested,

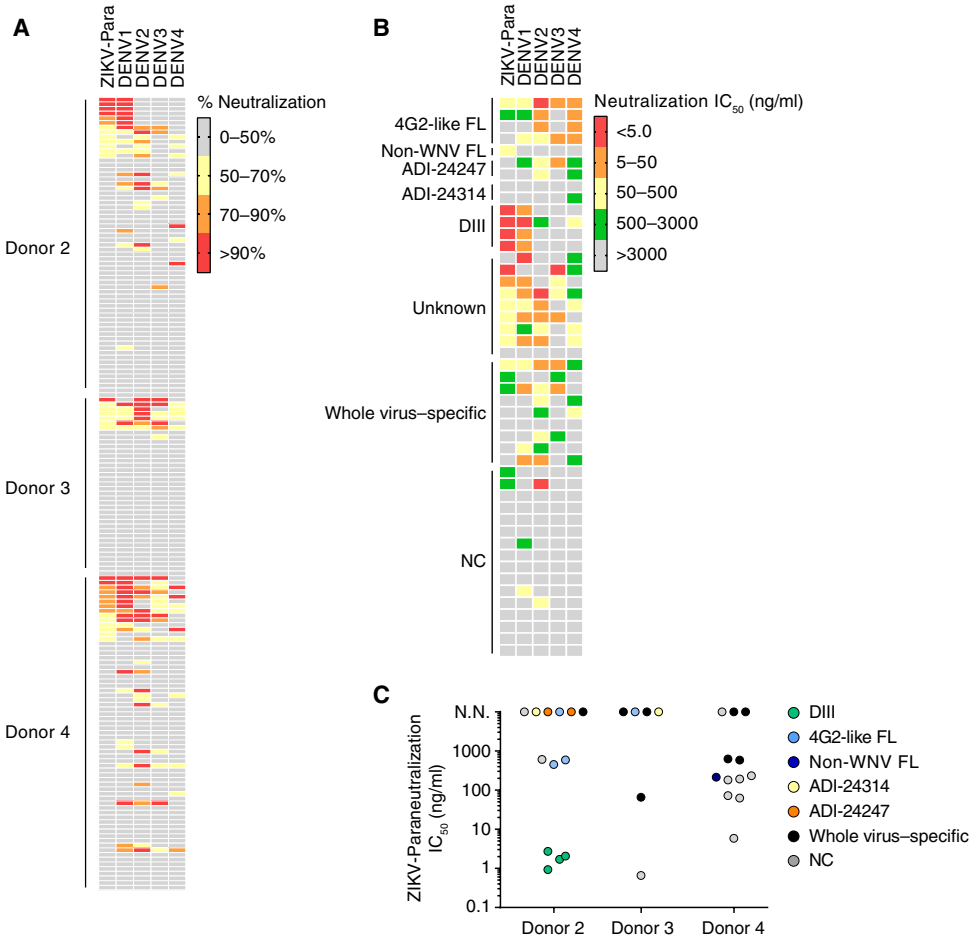

Fig. 3. Neutralizing activity of mAbs isolated from plasmablasts during acute ZIKV infection in DENV-experienced donors. (**A**) Heat map showing mAb neutralization of ZIKV-Para, DENV1, DENV2, DENV3, and DENV4 at a concentration of 1.0 μg/ml. (**B**) Heat map showing neutralization IC_{50}s for selected mAbs against ZIKV-Para, DENV1, DENV2, DENV3, and DENV4. Epitope assignments are indicated on the left. (**C**) Neutralization IC_{50}s for selected mAbs against ZIKV-Para. IC_{50} values represent the concentration of IgG required to reduce viral infectivity by 50%. Neutralization assays were performed using a live virus plaque reduction assay. N.N., non-neutralizing.

as defined by the area under the curve (fig. S10). Together, the results show that the acute B cell response to ZIKV in DENV-immune donors is dominated by cross-reactive antibodies that show poorly neutralizing activity and a propensity to enhance ZIKV infection in vitro.

Isolation of E-specific mAbs from longitudinal samples obtained from the DENV-experienced donors

To track the evolution of the B cell response to ZIKV in DENV-experienced donors, we collected blood samples from donors 2, 3, and 4 about 5 months after infection (table S1). To assess the magnitude of the E-specific memory B cell response at this time point, we stained peripheral B cells with a fluorescently labeled ZIKV E protein and analyzed them by flow cytometry (Fig. 4A and fig. S11). Robust E-specific memory B cell responses were observed in donors 3 and 4, whereas E-specific memory B cells were undetectable in donor 2 (Fig. 4A). The reasons for this are unclear, but given that donor 2 showed the highest frequency of plasmablasts during acute infection, one explanation is that the virus was rapidly cleared by the plasmablast-derived antibodies, which prevented the formation of a germinal center (GC) response. Four hundred ZIKV E–specific memory B cells were single cell–sorted from donors 3 and 4, and about 200 V_H and V_L pairs were cloned and expressed as full-length IgGs for further characterization. To assess the extent of affinity maturation that occurred over this time period, the apparent binding affinities of the E-specific memory B cell–derived mAbs were measured and compared with the affinities of the E-specific plasmablast-derived mAbs. As expected, the average apparent affinity for ZIKV E was significantly higher in the memory B cell subset, suggesting that the ZIKV-induced B cells underwent affinity maturation over time (Fig. 4B). Clonal expansions were observed in both donor response repertoires (Fig. 4C), but there were few to no clonal lineages shared between the plasmablast and memory B cell–derived subsets (table S9 and fig. S12). Although the sampling size is too small to determine the degree of overlap between the two B cell populations, these results suggest that the most dominant clonal lineages likely differ between the two compartments.

ZIKV infection induces de novo and cross-reactive memory B cell responses in DENV-experienced donors

We next assessed the degree of cross-reactivity with the E proteins from DENV1–4. Unexpectedly, 60 and 30% of memory B cell–derived mAbs from donors 3 and 4, respectively, bound exclusively to ZIKV E, suggesting that these antibodies either arose from preexisting memory B cells that uniformly lost DENV reactivity during the process of affinity maturation or originated from activated naïve B cells that had entered GCs and undergone affinity maturation (Fig. 4D and table S8). In support of the latter hypothesis, sequence analysis revealed no overall increase in SHM in the ZIKV-specific memory B cell–derived mAbs compared with the plasmablast-derived mAbs (Fig. 4E). Epitope mapping experiments showed that about 10 to 20% of the ZIKV-specific memory B cell–derived mAbs bound to epitopes within DIII, 0 to 15% bound to epitopes within or proximal to the FL, and 0 to 2% bound to epitopes overlapping that of ADI-24314 (fig. S13 and table S8). To estimate the number of different antigenic sites recognized by the remaining ZIKV-specific mAbs, we performed competitive binding assays with two mAbs from the panel (ADI-30056 and ADI-30023) that did not compete with ZV-67, 4G2, ADI-24314, ADI-24247, or each other (table S8). On the basis of these results, we found that 50 to 60% of the ZIKV-specific mAbs targeted unknown sites defined by ADI-30056 or ADI-30023 and 10 to

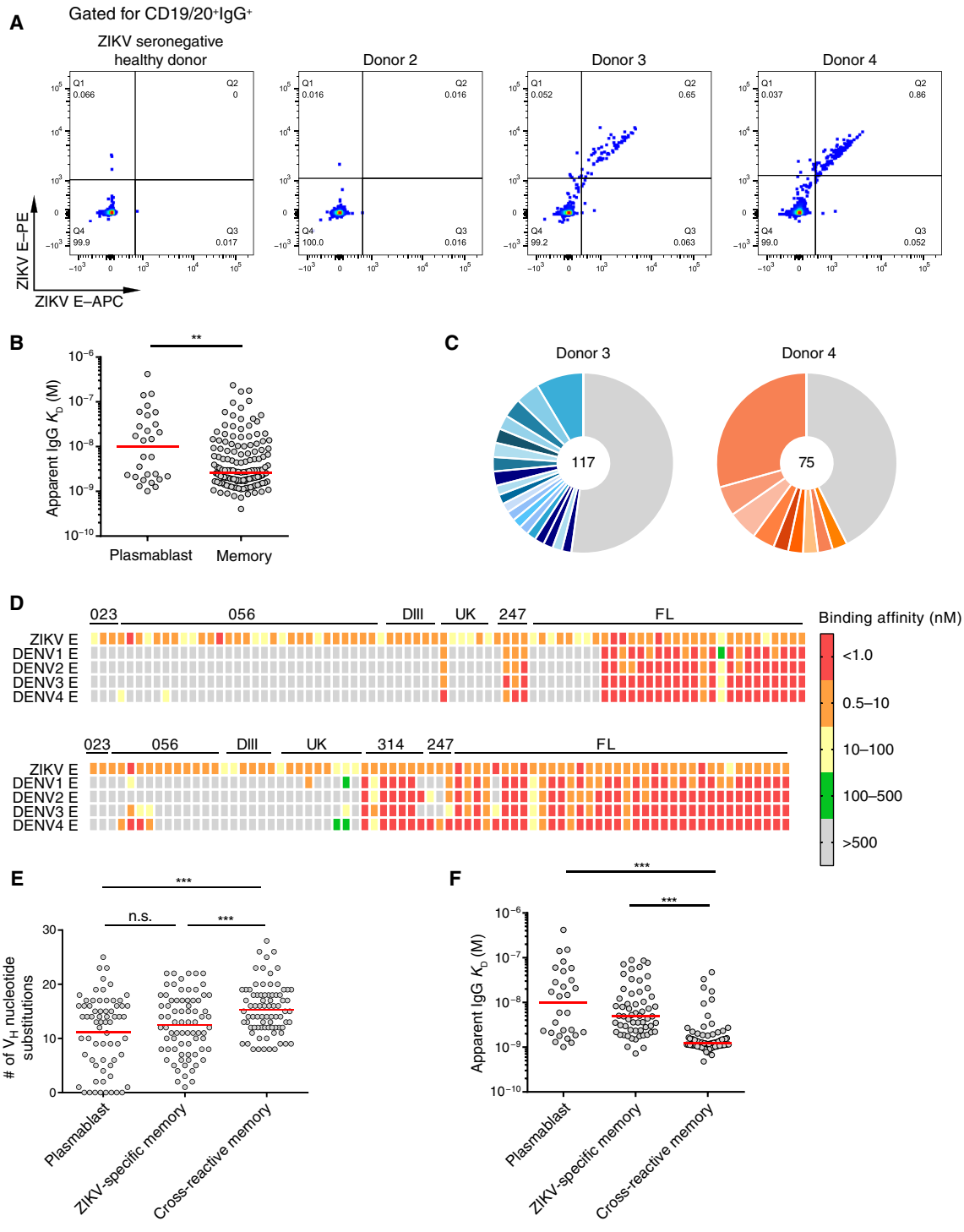

Fig. 4. Longitudinal analysis of ZIKV E–specific memory B cell responses in the DENV-experienced donors. (**A**) ZIKV E–specific memory B cell sorting. Fluorescence-activated cell sorting (FACS) plots show ZIKV E reactivity of IgG^+ B cells from the three convalescent DENV-experienced donors and a ZIKV seronegative healthy donor control. B cells in quadrant 2 (Q2) were single cell–sorted for mAb cloning. ZIKV E was labeled with two different colors to reduce background binding. (**B**) Apparent binding affinities of plasmablast and memory B cell–derived mAbs to recombinant ZIKV E. Red bars indicate the median IC_{50}s. (**C**) Clonal lineage analysis of memory B cell–derived mAbs. Heavy-chain sequences were assigned to lineages using Clonify (*52*). Each lineage is represented as a segment proportional to the lineage size. The total number of recovered heavy chains is shown in the center of each pie. All lineages that contain only a single sequence are combined and shown as a single gray segment. (**D**) Heat map showing apparent binding affinities of the memory B cell–derived mAbs to recombinant ZIKV E and DENV1–4 E proteins. Top: mAbs cloned from donor 3. Bottom: mAbs cloned from donor 4. 023, ADI-30023 competitor; 056, ADI-30056 competitor; 314, ADI-24314 competitor; 247, ADI-24247 competitor; FL, 4G2 competitor; DIII, recombinant DIII binder; UK, unknown. (**E**) Load of somatic mutations (expressed as the number of nucleotide substitutions in the V_H) in mAbs isolated from plasmablasts and memory B cells in DENV-experienced donors. Each point represents an individual mAb. Red bars indicate the median number of nucleotide substitutions. (**F**) Binding of plasmablast and memory B cell–derived mAbs to recombinant ZIKV E. Apparent binding affinities are shown in the plot. Red bars indicate median apparent IC_{50}s. Statistical comparisons were made using Mann-Whitney test (***$P < 0.001$, **$P < 0.01$; n.s., not significant).

30% of mAbs did not compete with any of the control mAbs (fig. S13 and table S8).

The majority (84%) of DENV cross-reactive mAbs showed reactivity with all four DENV serotypes (Fig. 4D and table S8). Most of these broadly cross-reactive mAbs showed DENV-biased binding profiles and overall higher levels of SHM compared with the ZIKV-specific mAbs, suggesting that they likely arose from preexisting DENV-induced memory B cells that formed secondary GCs (Fig. 4,

D and E, and table S8). The latter result also provides additional evidence that the ZIKV-specific mAbs originated from naïve B cells that underwent affinity maturation rather than from preexisting memory B cells that lost DENV cross-reactivity. In addition, the average apparent affinity of the cross-reactive mAbs was significantly higher than those of the plasmablast-derived mAbs and the ZIKV-specific memory B cell–derived mAbs, providing further evidence for GC reentry by memory B cells (Fig. 4F). This result is consistent with recent studies in mice demonstrating that memory B cells can rediversify their B cell receptors within secondary GCs (*33*–*35*). As anticipated based on their broad cross-reactivity, most of these mAbs targeted epitopes within or proximal to the FL on DII (Fig. 4D and table S8).

We next tested the memory B cell–derived mAbs for neutralizing activity. Only a small minority of the cross-reactive mAbs (4 of 80 or 5%) showed neutralizing activity against ZIKV-Para at a concentration of 1 μg/ml, whereas the overwhelming majority (52 of 73 or 71%) of the ZIKV-specific mAbs showed such neutralizing activity (Fig. 5A and table S8). Neutralization titration experiments revealed that most potent ZIKV-specific mAbs displayed IC_{50}s between 1.0 and 10 ng/ml and targeted epitopes overlapping that of ADI-30056 (Fig. 5B and table S10). About 90% of the cross-reactive mAbs tested showed more potent neutralizing activity against at least one of the four DENV serotypes than ZIKV-Para, further suggesting that these mAbs originated from preexisting memory B cells that reentered GCs (Fig. 5C and table S10). We conclude that the ZIKV-induced memory B cell response is composed of both OAS-phenotype antibodies that display broad cross-reactivity and poorly neutralizing activity, and de novo generated ZIKV-specific antibodies that show potent but type-specific neutralizing activity.

DISCUSSION

Here, we have used single B cell cloning and large-scale antibody characterization to track the evolution of ZIKV-induced B cell responses in three DENV-experienced donors. In all three donors, massive plasmablast populations were observed during acute ZIKV infection, which were similar in magnitude to the plasmablast responses previously observed in individuals experiencing secondary DENV infection (*24*). The plasmablast population in a ZIKV-infected, DENV-naïve donor was relatively small, which could be due to multiple factors, such as differences in age, viral load, or immune history. However, the immune history explanation is consistent with previous studies that have shown that peripheral blood plasmablast responses during primary infection are delayed and substantially lower in magnitude than during secondary infection (*36*, *37*). The plasmablast responses in the three DENV-experienced donors were clonally expanded and showed relatively high levels of SHM—consistent with a recall response dominated by reactivated memory B cells—whereas the plasmablasts from the ZIKV-infected, DENV-naïve donor showed substantially lower levels of SHM and somewhat more limited clonal expansion, suggesting emergence via activation of naïve B cells. Over half of the plasmablast-derived mAbs isolated from the DENV-experienced donors showed reactivity with whole ZIKV particles or recombinant ZIKV NS1, whereas a substantially smaller fraction of the plasmablast-derived mAbs from the DENV-naïve donor showed such binding. This result could be either due to the low binding affinity of mAbs isolated from activated naïve B cells or that the plasmablast response in this donor was largely directed against viral antigens that were not tested in this study.

Binding and functional characterization of the plasmablast-derived mAbs from donors 2, 3, and 4 revealed that the acute B cell response to ZIKV is dominated by reactivated DENV clones, thus providing evidence of OAS during the acute-phase B cell response to ZIKV in DENV-experienced donors. Most of these antibodies, although broadly cross-reactive, displayed poorly neutralizing activity and enhanced ZIKV infection in vitro, suggesting that preexisting immunity to DENV virus may negatively affect early protective B cell responses to ZIKV. None of the mAbs isolated from the ZIKV-infected DENV-naïve donor showed cross-reactivity with any of the four serotypes of DENV, suggesting that highly conserved epitopes are not immunodominant in the context of primary ZIKV infection. Although ADE has been proposed to be primarily driven by

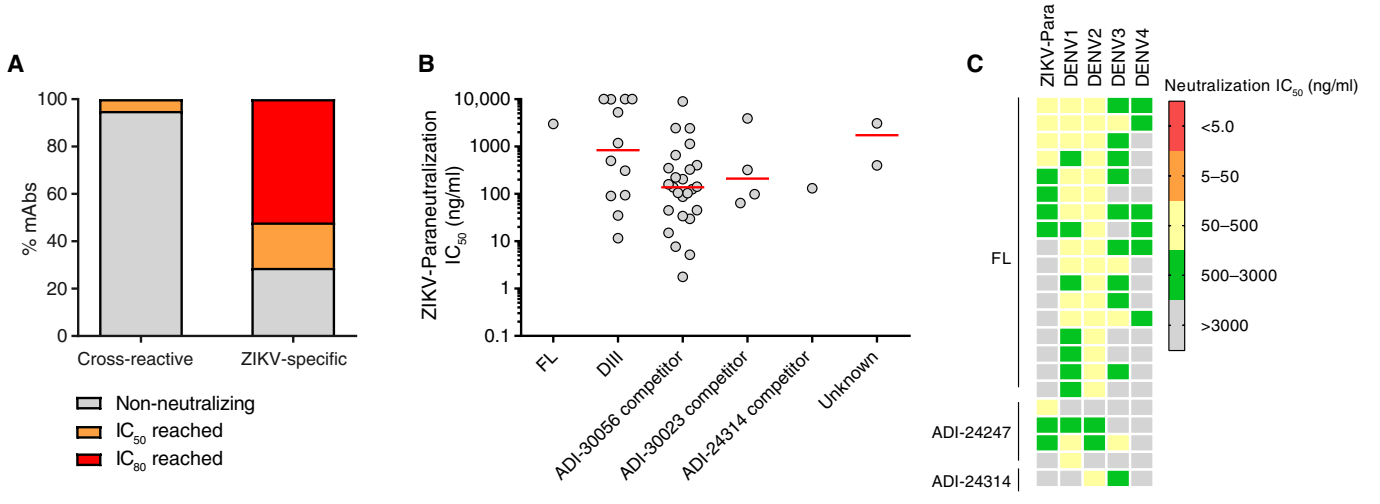

Fig. 5. Neutralizing activity of memory B cell–derived mAbs. (**A**) Percentage of cross-reactive and ZIKV-specific mAbs that reached neutralization IC_{50} or IC_{80} at a concentration of 1.0 μg/ml. (**B**) Neutralization IC_{50} values of selected mAbs from each competition group. IC_{50} values represent the concentration of IgG required to reduce viral infectivity by 50%. Red bars indicate median IC_{50}s. (**C**) Heat map showing neutralization IC_{50}s for selected cross-reactive mAbs against ZIKV-Para, DENV1, DENV2, DENV3, and DENV4. Neutralization assays were performed using a live virus plaque reduction assay.

preexisting serum antibody, plasmablasts secrete substantial amounts of antibody during acute infection. It is therefore possible that boosting of poorly neutralizing responses during the early stages of infection could contribute to ADE. However, it is important to emphasize that although animal studies have suggested a role for ADE in vivo (*14*), the relevance of ADE in determining the severity and/or higher risk for ZIKV infection remains yet to be elucidated in humans.

Although most of the plasmablast-derived mAbs isolated from the three DENV-experienced donors were poorly neutralizing, a subset of mAbs from donor 2 showed highly potent neutralizing activity against both ZIKV and DENV1. These mAbs bound to epitopes within the lateral ridge of DIII and showed convergent sequence signatures in both the heavy and light chains. Similar antibodies were recently isolated from several DENV-immune donors that were selected on the basis of high ZIKV neutralizing titers (*38*). The identification of recurrent potent nAbs in multiple different donors suggests that this antigenic region may be a particularly attractive target for vaccines intended for DENV-immune populations. Despite the identification of potent nAbs from the donor 2 plasmablast population, the acute serum from this donor showed weaker neutralizing activity than the acute sera from donors 3 and 4. One possible explanation for this result is that the donor 3 and 4 sera contain overall higher titers of anti-ZIKV antibodies compared with the donor 2 serum. In support of this hypothesis, the donor 2 acute serum showed substantially weaker binding to whole DENV and ZIKV particles compared with the acute serum from donors 3 and 4.

The phenomenon of OAS has been documented in the context of repeated influenza virus exposure as well as during secondary DENV infections (*17*, *39*–*43*), and these studies have suggested that memory responses to the primary infecting strain may prevent the induction of effective de novo responses. Our results show that the ZIKV-induced memory B cell response in DENV-experienced donors is composed of both poorly neutralizing OAS-phenotype antibodies—which appear to have originated from preexisting DENV-induced memory B cells that reentered GCs—and potently neutralizing ZIKV-specific antibodies that likely originated from naïve B cells that entered primary GCs. Hence, our results suggest that effective de novo memory B cell responses to ZIKV can be induced in the presence of preexisting cross-reactive DENV clones. However, only about 50% of the mAbs isolated from E-specific memory B cells were ZIKV-specific; the remaining mAbs were broadly cross-reactive, poorly neutralizing, and potently enhancing. The relative contribution of these two different classes of antibodies to protection, virulence, and immunopathology of ZIKV infection remains to be elucidated.

One limitation of our study is the small number of donors studied. As a result, intradonor comparisons can be made with high certainty, but interdonor comparisons are less robust. However, we found evidence of OAS in all three DENV-experienced donors, suggesting that this phenomenon likely occurs in most ZIKV-infected donors that have been previously exposed to DENV. Another limitation of our study was the use of recombinant ZIKV E for memory B cell sorting, which prevented the isolation of memory B cell–derived mAbs that recognize quaternary epitopes. Last, because we were not able to obtain detailed medical histories for these donors, it was not possible to determine the number and frequency of previous DENV infections and the number of DENV serotypes to which they had been exposed. However, the serological data strongly suggest that donors 2, 3, and 4 had experienced at least one DENV infection before ZIKV infection, which we believe is sufficient for the interpretation of the results of this study.

Although our study was performed using naturally infected donors, vaccines expressing full-length ZIKV E—which include multiple recently described plasmid DNA, purified inactivated, protein subunit, adenovirus vector, and mRNA vaccines (*44*–*49*)—would be expected to induce similar responses in DENV-experienced individuals. Such vaccines, which will need to be deployed in areas that are highly endemic for DENV, will likely induce a substantial OAS response in these individuals. Given this possibility, the clinical development of ZIKV vaccines should also consider the recruitment and immunization of DENV-immune donors. Ongoing phase 1 studies on ZIKV vaccine candidates are currently being performed on individuals living in areas that are not endemic for DENV, and therefore, most of these individuals are likely DENV-naïve. Together, the results of this study provide rationale for the design of vaccines specifically focused on the DIII lateral ridge or other ZIKV-specific neutralizing epitopes for use in DENV-immune populations.

MATERIALS AND METHODS

Study design

We initiated this study to gain an in-depth understanding of the antibody response to ZIKV in DENV-experienced donors. To study these responses, we obtained peripheral blood mononuclear cells (PBMCs) from three ZIKV-infected donors that had serological evidence or previous DENV exposure and one ZIKV-infected naïve donor for comparison. Four donors were included in this study because this was the largest number of donors for which large numbers of antibodies could be practically cloned and characterized. At least two independent experiments were performed for affinity measurements, neutralization assays, enhancement assays, and antibody competition assays, and the results shown are derived from single representative experiments. All samples for this study were collected with informed consent of volunteers. This study was unblinded and not randomized.

PBMC and plasma isolation

Blood and serum samples were obtained through Antibody Systems Inc. under the Scripps Research Institute IRB-15-6683. PBMCs were isolated as previously described (*50*). Briefly, whole blood was diluted 1:2 with phosphate-buffered saline (PBS) and underwent ultracentrifugation over layered Lymphoprep (STEMCELL Technologies). PBMC monolayer was collected, resuspended, and stored in liquid nitrogen.

Generation of ZIKV and DENV viruses

Vero cells were cultured in minimal essential medium (MEM) (Corning Cellgro) containing 5% heat-inactivated fetal bovine serum (Gibco-Invitrogen). Viruses were supplied by D. Watkins and included Zika-Paraiba 2015, DENV1 Western Pacific U88535.1, DENV2 NGC AF038403.1, DENV3 Selman/78 AY648961, and DENV4 AF326825.1. Vero cells were infected with each virus and maintained until 50% reduction in viability was observed, after which supernatant was collected, filtered, and stored at −80°C.

Antibody sequencing

Reverse transcription and subsequent PCR amplification of V_H and V_L genes were performed using SuperScript III (Life Technologies) according to published protocols (*51*). All PCRs were performed in

25-ml volume with 2.5 ml of complementary DNA (cDNA) transcript using HotStarTaq DNA polymerase master mix (Qiagen) and mixtures of previously described primers (*51*). Second-round nested PCRs were performed using Phusion proofreading polymerase (New England Biolabs). Two additional rounds of PCR were performed using primers with barcodes specific to the plate number and well location as well as adapters appropriate for sequencing on an Illumina MiSeq. This reaction was performed in a 25-ml volume with HotStarTaq DNA polymerase master mix (Qiagen). Amplified IgG V_H and V_L genes were sequenced on an Illumina MiSeq (600-base v3 reagent kit; Illumina), and reads corresponding to the same plate per well location were combined into consensus sequences. Germline assignment was performed with AbStar (https://github.com/briney/abstar), and clonal lineages were assigned with Clonify (*52*).

Western blots

Whole-virus ZIKV lysate, whole-virus DENV lysate, and recombinant E protein (catalog no. R01635, Meridian Life Science) were separated by SDS–polyacrylamide gel electrophoresis under reducing conditions in 4 to 20% gels (Bio-Rad) to polyvinylidene difluoride membranes (Thermo Fisher Scientific). Membranes were blocked overnight at 4°C in 5% nonfat dry milk in tris-buffered saline (TBS) containing 0.05% Tween 20 (TBS-T). Subsequently, membranes were incubated with 1:2000 dilution of mAb in 10 ml of TBS-T containing 5% milk for 1 hour and washed three times with TBS-T. The secondary antibody used to detect 4G2 was a horseradish peroxidase (HRP)–conjugated goat polyclonal secondary antibody to mouse IgG (Abcam), and the secondary antibody used to detect human mAbs was an HRP-conjugated goat polyclonal secondary antibody to human IgG (Abcam). Secondary antibodies were diluted 1:2000 in 10 ml of TBS-T with 5% milk and applied to the membrane for 1 hour, and then the membrane was washed three times with TBS-T and developed with HRP development solution (Bio-Rad).

Focus reduction neutralization test

Virus-specific nAb responses were titrated essentially as previously described (*53*). Briefly, antibody was diluted serially in MEM (Corning Cellgro) containing 5% heat-inactivated fetal bovine serum (Gibco-Invitrogen) and incubated for 1 hour at 37°C with virus. The initial dilution tested for all mAbs was 10 μg/ml, and threefold dilutions were performed. After incubation, the antibody-virus mixture was added in triplicate to 96-well plates containing 80% confluent monolayers of Vero E6 cells. Plates were incubated for 1.5 hours at 37°C. After the incubation, wells were overlaid with 1% methylcellulose in supplemented MEM with 2% heat-inactivated fetal bovine serum (Gibco-Invitrogen) and 1:100 Hepes. Plates were incubated at 37°C and 5% CO_2 for 40 hours, after which cells were fixed and permeabilized with Perm/Wash buffer (BD Biosciences) for 5 min. After permeabilization, cells were incubated with 1:2000 dilution of anti-flavivirus antibody (MAB10216) for 2 hours and then washed with PBS (EMD Millipore). After washing, the cells were incubated with anti-mouse HRP-conjugated secondary antibody (Sigma) in Perm/Wash buffer for 2 hours. After washing of cells with PBS, plates were developed with peroxidase substrate (KPL). All viruses were titered to yield 100 plaques per well in the absence of neutralization and fixed at 40 hours to prevent plaque spread or overlap. Experiments were performed in triplicate. Neutralization IC_{50}s were determined using GraphPad Prism software. One site - Fit $logIC_{50}$ was used with the following model: $Y = \text{Bottom} + (\text{Top} - \text{Bottom})/(1 + 10\text{^}(X - \text{LogIC}_{50}))$. The top and bottom of the curves were constrained to values of 100 and 0. The IC_{50} was then defined from the best-fit curve for each antibody as defined by the concentration that resulted in 50% reduction in foci number.

Serum ELISAs

For NS1 ELISAs, plates were coated with NS1 proteins (5 μg/ml) diluted in PBS and incubated overnight at 4°C. Wells were washed and then blocked with 3% bovine serum albumin (BSA) in PBS for 1 hour at 37°C. Wells were washed, and serial dilutions of human plasma diluted in 1% BSA and 0.05% Tween 20 were added and incubated for 1 hour at 37°C. Wells were washed, and alkaline phosphatase (AP)–conjugated goat anti-human IgG (Jackson ImmunoResearch) secondary antibody was added and incubated for 1 hour at 37°C. Wells were washed twice and developed with *para*-nitrophenylphosphate in 1× diethanolamine. Plates were read on a SpectraMax microplate reader (Molecular Devices) at 405-nm wavelength. For virus binding, ELISA plates were coated with 4G2 (10 μg/ml) (Millipore, MAB10216) diluted in PBS and incubated overnight at 4°C. After washing, wells were blocked with 3% BSA in PBS for 1 hour at 37°C. After removal of the blocking solution, whole ZIKV or DENV particles diluted in 1% BSA and 0.05% Tween 20 were applied to the plates and incubated at 37°C for 1 hour. After washing, serum was titrated and incubated at 37°C for 1 hour. The wells were washed, and AP-conjugated goat anti-human IgG (Jackson ImmunoResearch) secondary antibody was added and incubated for 1 hour at 37°C. Wells were washed twice and developed with *para*-nitrophenylphosphate in 1× diethanolamine. Plates were read on a SpectraMax microplate reader (Molecular Devices) at 405-nm wavelength.

mAb binding ELISAs

ELISA plates were coated with 4G2 (10 μg/ml) (Millipore MAB10216) diluted in PBS and incubated overnight at 4°C. After washing, wells were blocked with 3% BSA in PBS for 1 hour at 37°C. After removal of the blocking solution, 10^4 plaque-forming units of unpurified ZIKV or DENV particles diluted in 1% BSA and 0.05% Tween 20 was added to each well of the ELISA plate and incubated at 37°C for 1 hour. After washing, mAbs were either titrated or added at a concentration of 10 μg/ml and incubated at 37°C for 1 hour. Wells were washed, and AP-conjugated goat anti-human IgG (Jackson ImmunoResearch) secondary antibody was added and incubated for 1 hour at 37°C. Wells were washed twice and developed with *para*-nitrophenylphosphate in 1× diethanolamine. Plates were read on a SpectraMax microplate reader (Molecular Devices) at 405-nm wavelength.

Single B cell sorting

For plasmablast sorting, PBMCs were stained using anti-human CD38 (fluorescein isothiocyanate), CD27 [phycoerythrin (PE)–Cy7], CD20 (BUV737), CD3 [allophycocyanin (APC)–Cy7], CD8 (APC-Cy7), and CD14 (APC-H7). Plasmablasts were defined as $CD19^+CD3^-CD20^{-/lo}CD27^{hi}CD38^{hi}$. For memory B cell sorting, purified B cells were stained using anti-human IgG [Brilliant Violet (BV) 605], CD27 (BV421), CD8 [peridinin chlorophyll protein (PerCP)–Cy5.5], CD14 (PerCP-Cy5.5), CD19 (PE-Cy7), CD20 (PE-Cy7), and a mixture of dual-labeled ZIKV E tetramers (50 nM each). Single cells were sorted on a BD FACSAria II into 96-well PCR plates (Bio-Rad) containing 20 μl of lysis buffer per well [5 μl of 5× first-strand cDNA buffer (Invitrogen), 0.25 μl of RNaseOUT (Invitrogen), 1.25 μl of dithiothreitol (Invitrogen), 0.625 μl of NP-40 (New England Biolabs), and 12.6 μl of deionized H_2O].

Plates were immediately frozen on dry ice before storage at −80°C. Flow cytometry data were analyzed using FlowJo software.

Amplification and cloning of antibody variable genes

Single B cell PCR was performed essentially as previously described (*51*). Briefly, IgH, Igλ, and Igκ variable gene transcripts were amplified by reverse transcription PCR and nested PCRs using cocktails of primers specific for IgG (*51*). The primers used in the second round of PCR contained 40 base pairs of 5′ and 3′ homology to the cut expression vectors to allow for cloning by homologous recombination into *Saccharomyces cerevisiae* (*54*). PCR products were cloned into *S. cerevisiae* using the lithium acetate method for chemical transformation (*55*). Each transformation reaction contained 20 μl of unpurified heavy-chain and light-chain PCR product and 200 ng of cut heavy-chain and light-chain plasmids. Individual yeast colonies were picked for sequencing and downstream characterization.

Expression and purification of antibodies

Antibodies used for binding experiments, competition assays, neutralization assays, and structural studies were expressed in *S. cerevisiae* cultures grown in 24-well plates (*54*). After 6 days of growth, the yeast cell culture supernatant was harvested by centrifugation and subject to purification. Cell supernatants were purified by passing over Protein A agarose (MabSelect SuRe from GE Healthcare Life Sciences). The bound antibodies were washed with PBS, eluted with 200 mM acetic acid/50 mM NaCl (pH 3.5) into one-eighth volume of 2 M Hepes (pH 8.0), and buffer-exchanged into PBS (pH 7.0). Fab fragments were generated by digesting the IgGs with papain for 2 hours at 30°C. The digestion was terminated by the addition of iodoacetamide, and the Fab and Fc mixtures were passed over Protein A agarose to remove Fc fragments and undigested IgG. The flowthrough of the Protein A resin was then passed over CaptureSelect IgG-CH1 affinity resin (Thermo Fisher Scientific) and eluted with 200 mM acetic acid/50 mM NaCl (pH 3.5) into one-eighth volume of 2 M Hepes (pH 8.0). Fab fragments then were buffer-exchanged into PBS (pH 7.0).

BLI binding analysis

IgG binding affinities were determined by BLI measurements using a FortéBio Octet HTX instrument (Pall Life Sciences). For high-throughput binding affinity screening, IgGs were immobilized on AHQ sensors (Pall Life Sciences) and exposed to 100 nM ZIKV E (Meridian Life Science Inc.), DENV1–4 E (Native Antigen Company), or NS1 proteins (Native Antigen Company) in PBS containing 0.1% BSA (PBSF) for an association step, followed by a dissociation step in PBSF buffer. Data were analyzed using the FortéBio Data Analysis Software 7. The data were fit to a 1:1 binding model to calculate an association and dissociation rate, and binding K_Ds (equilibrium dissociation constants) were calculated using the ratio k_d (dissociation constant)/k_a (association constant).

Antibody competition assays

Antibody competition assays were performed as previously described (*54*). Antibody competition was measured by the ability of a control anti-ZIKV E Fab to inhibit binding of yeast surface–expressed anti-ZIKV E IgGs to ZIKV E (Meridian Life Science Inc.). Biotinylated ZIKV E (50 nM) was preincubated with 1 μM competitor Fab for 30 min at room temperature and then added to a suspension of yeast-expressed anti-ZIKV E IgG. After 5-min incubation, unbound antigen was removed by washing with PBSF. After washing, bound antigen was detected using streptavidin–Alexa Fluor 633 (Life Technologies) at a 1:500 dilution and analyzed by flow cytometry using a BD FACSCanto II. Results are expressed as the fold reduction in antigen binding in the presence of competitor Fab relative to an antigen-only control.

Statistical analyses

All statistical analyses were performed using GraphPad Prism. Statistical significance was determined using an unpaired nonparametric Mann-Whitney test or Kruskal-Wallis test. *P* values less than 0.05 were considered significant.

SUPPLEMENTARY MATERIALS

immunology.sciencemag.org/cgi/content/full/2/14/eaan6809/DC1

Fig. S1. Binding of acute serum to ZIKV and DENV1–4 viral particles and NS1 proteins.
Fig. S2. Plasmablast sorting.
Fig. S3. Binding of plasmablast-derived mAbs to ZIKV-Para by ELISA.
Fig. S4. Western blot analysis of mAb binding to ZIKV lysate.
Fig. S5. Heat map of mAb binding reactivity to recombinant ZIKV E, WNV E, DIII, and E-FL.
Fig. S6. mAb binding to recombinant ZIKV and DENV E proteins.
Fig. S7. ELISA binding of whole virus–specific clones to ZIKV and DENV.
Fig. S8. SHM of NS1-specific mAbs.
Fig. S9. Representative neutralization curves.
Fig. S10. Enhancement of ZIKV infection by plasmablast-derived mAbs isolated from DENV-experienced donors.
Fig. S11. Memory B cell sorting.
Fig. S12. Distribution of clonal lineage members across plasmablast and memory B cell subsets.
Fig. S13. Epitope mapping of ZIKV-specific mAbs derived from memory B cells.
Table S1. Clinical characteristics of ZIKV-infected donors.
Table S2. Binding properties of ZIKV E–specific mAbs isolated from plasmablasts.
Table S3. Binding characteristics of mAb 4G2.
Table S4. Sequences of ZV-67 competitor mAbs.
Table S5. Competition of ADI-24247 and ADI-24314 with each other and with control mAbs.
Table S6. Binding properties of NS1-specific mAbs isolated from plasmablasts.
Table S7. Neutralizing activity of selected plasmablast-derived mAbs.
Table S8. Binding properties of ZIKV E–specific mAbs isolated from memory B cells.
Table S9. Clonal lineages shared between plasmablast and memory B cell–derived antibodies.
Table S10. Neutralizing activity of selected memory B cell–derived mAbs.

REFERENCES AND NOTES

1. J. Mlakar, M. Korva, N. Tul, M. Popović, M. Poljšak-Prijatelj, J. Mraz, M. Kolenc, K. Resman Rus, T. Vesnaver Vipotnik, V. Fabjan Vodušek, A. Vizjak, J. Pižem, M. Petrovec, T. Avšič Županc, Zika virus associated with microcephaly. *N. Engl. J. Med.* **374**, 951–958 (2016).
2. V.-M. Cao-Lormeau, A. Blake, S. Mons, S. Lastère, C. Roche, J. Vanhomwegen, T. Dub, L. Baudouin, A. Teissier, P. Larre, A.-L. Vial, C. Decam, V. Choumet, S. K. Halstead, H. J. Willison, L. Musset, J.-C. Manuguerra, P. Despres, E. Fournier, H.-P. Mallet, D. Musso, A. Fontanet, J. Neil, F. Ghawché, Guillain-Barré Syndrome outbreak associated with Zika virus infection in French Polynesia: A case-control study. *Lancet* **387**, 1531–1539 (2016).
3. D. Sirohi, Z. Chen, L. Sun, T. Klose, T. C. Pierson, M. G. Rossmann, R. J. Kuhn, The 3.8 Å resolution cryo-EM structure of Zika virus. *Science* **352**, 467–470 (2016).
4. G. Barba-Spaeth, W. Dejnirattisai, A. Rouvinski, M.-C. Vaney, I. Medits, A. Sharma, E. Simon-Lorière, A. Sakuntabhai, V.-M. Cao-Lormeau, A. Haouz, P. England, K. Stiasny, J. Mongkolsapaya, F. X. Heinz, G. R. Screaton, F. A. Rey, Structural basis of potent Zika–dengue virus antibody cross-neutralization. *Nature* **536**, 48–53 (2016).
5. W. Dejnirattisai, P. Supasa, W. Wongwiwat, A. Rouvinski, G. Barba-Spaeth, T. Duangchinda, A. Sakuntabhai, V.-M. Cao-Lormeau, P. Malasit, F. A. Rey, J. Mongkolsapaya, G. R. Screaton, Dengue virus sero-cross-reactivity drives antibody-dependent enhancement of infection with zika virus. *Nat. Immunol.* **17**, 1102–1108 (2016).
6. L. Priyamvada, K. M. Quicke, W. H. Hudson, N. Onlamoon, J. Sewatanon, S. Edupuganti, K. Pattanapanyasat, K. Chokephaibulkit, M. J. Mulligan, P. C. Wilson, R. Ahmed, M. S. Suthar, J. Wrammert, Human antibody responses after dengue virus infection are highly cross-reactive to Zika virus. *Proc. Natl. Acad. Sci. U.S.A.* **113**, 7852–7857 (2016).
7. K. Stettler, M. Beltramello, D. A. Espinosa, V. Graham, A. Cassotta, S. Bianchi, F. Vanzetta, A. Minola, S. Jaconi, F. Mele, M. Foglierini, M. Pedotti, L. Simonelli, S. Dowall, B. Atkinson, E. Percivalle, C. P. Simmons, L. Varani, J. Blum, F. Baldanti, E. Cameroni, R. Hewson, E. Harris, A. Lanzavecchia, F. Sallusto, D. Corti, Specificity, cross-reactivity, and function of antibodies elicited by Zika virus infection. *Science* **353**, 823–826 (2016).

8. S. B. Halstead, Neutralization and antibody-dependent enhancement of dengue viruses. *Adv. Virus Res.* **60**, 421–467 (2003).
9. S. C. Kliks, S. Nimmanitya, A. Nisalak, D. S. Burke, Evidence that maternal dengue antibodies are important in the development of dengue hemorrhagic fever in infants. *Am. J. Trop. Med. Hyg.* **38**, 411–419 (1988).
10. C. P. Simmons, T. N. B. Chau, T. T. Thuy, N. M. Tuan, D. M. Hoang, N. T. Thien, L. B. Lien, N. T. Quy, N. T. Hieu, T. T. Hien, C. McElnea, P. Young, S. Whitehead, N. T. Hung, J. Farrar, Maternal antibody and viral factors in the pathogenesis of dengue virus in infants. *J. Infect. Dis.* **196**, 416–424 (2007).
11. A. B. Kawiecki, R. C. Christofferson, Zika virus-induced antibody response enhances dengue virus serotype 2 replication in vitro. *J. Infect. Dis.* **214**, 1357–1360 (2016).
12. P. M. S. Castanha, E. J. M. Nascimento, C. Braga, M. T. Cordeiro, O. V. de Carvalho, L. R. de Mendonça, E. A. N. Azevedo, R. F. O. França, R. Dhalia, E. T. A. Marques Jr., Dengue virus (DENV)-specific antibodies enhance Brazilian Zika virus (ZIKV) infection. *J. Infect. Dis.* **2016**, 1–5 (2016).
13. A. P. Durbin, Dengue antibody and Zika: Friend or foe? *Trends Immunol.* **37**, 635–636 (2016).
14. S. V. Bardina, P. Bunduc, S. Tripathi, J. Duehr, J. J. Frere, J. A. Brown, R. Nachbagauer, G. A. Foster, D. Krysztof, D. Tortorella, S. L. Stramer, A. García-Sastre, F. Krammer, J. K. Lim, Enhancement of Zika virus pathogenesis by preexisting antiflavivirus immunity. *Science* **356**, 175–180 (2017).
15. D. A. Muller, P. R. Young, The flavivirus NS1 protein: Molecular and structural biology, immunology, role in pathogenesis and application as a diagnostic biomarker. *Antiviral Res.* **98**, 192–208 (2013).
16. M. Beltramello, K. L. Williams, C. P. Simmons, A. Macagno, L. Simonelli, N. T. H. Quyen, S. Sukupolvi-Petty, E. Navarro-Sanchez, P. R. Young, A. M. de Silva, F. A. Rey, L. Varani, S. S. Whitehead, M. S. Diamond, E. Harris, A. Lanzavecchia, F. Sallusto, The human immune response to Dengue virus is dominated by highly cross-reactive antibodies endowed with neutralizing and enhancing activity. *Cell Host Microbe* **8**, 271–283 (2010).
17. L. Priyamvada, A. Cho, N. Onlamoon, N.-Y. Zheng, M. Huang, Y. Kovalenkov, K. Chokephaibulkit, N. Angkasekwinai, K. Pattanapanyasat, R. Ahmed, P. C. Wilson, J. Wrammert, B cell responses during secondary dengue virus infection are dominated by highly cross-reactive, memory-derived plasmablasts. *J. Virol.* **90**, 5574–5585 (2016).
18. L. Li, S.-M. Lok, I.-M. Yu, Y. Zhang, R. J. Kuhn, J. Chen, M. G. Rossmann, The flavivirus precursor membrane-envelope protein complex: Structure and maturation. *Science* **319**, 1830–1834 (2008).
19. Y. Modis, S. Ogata, D. Clements, S. C. Harrison, Structure of the dengue virus envelope protein after membrane fusion. *Nature* **427**, 313–319 (2004).
20. G. Sapparapu, E. Fernandez, N. Kose, B. Cao, J. M. Fox, R. G. Bombardi, H. Zhao, C. A. Nelson, A. L. Bryan, T. Barnes, E. Davidson, I. U. Mysorekar, D. H. Fremont, B. J. Doranz, M. S. Diamond, J. E. Crowe, Neutralizing human antibodies prevent Zika virus replication and fetal disease in mice. *Nature* **540**, 443–447 (2016).
21. S. Bhatt, P. W. Gething, O. J. Brady, J. P. Messina, A. W. Farlow, C. L. Moyes, J. M. Drake, J. S. Brownstein, A. G. Hoen, O. Sankoh, M. F. Myers, D. B. George, T. Jaenisch, G. R. W. Wint, C. P. Simmons, T. W. Scott, J. J. Farrar, S. I. Hay, The global distribution and burden of dengue. *Nature* **496**, 504–507 (2013).
22. Y. Lustig, H. Zelena, G. Venturi, M. Van Esbroeck, C. Rothe, C. Perret, R. Koren, S. Katz-Likvornik, E. Mendelson, E. Schwartz, Sensitivity and kinetics of an NS1-based Zika virus enzyme-linked immunosorbent assay in Zika virus-infected travelers from Israel, the Czech Republic, Italy, Belgium, Germany, and Chile. *J. Clin. Microbiol.* **55**, 1894–1901 (2017).
23. D. Huzly, I. Hanselmann, J. Schmidt-Chanasit, M. Panning, High specificity of a novel Zika virus ELISA in European patients after exposure to different flaviviruses. *Euro Surveill.* **21**, 30203 (2016).
24. J. Wrammert, N. Onlamoon, R. S. Akondy, G. C. Perng, K. Polsrila, A. Chandele, M. Kwissa, B. Pulendran, P. C. Wilson, O. Wittawatmongkol, S. Yoksan, N. Angkasekwinai, K. Pattanapanyasat, K. Chokephaibulkit, R. Ahmed, Rapid and massive virus-specific plasmablast responses during acute dengue virus infection in humans. *J. Virol.* **86**, 2911–2918 (2012).
25. J. Wrammert, K. Smith, J. Miller, W. A. Langley, K. Kokko, C. Larsen, N.-Y. Zheng, I. Mays, L. Garman, C. Helms, J. James, G. M. Air, J. D. Capra, R. Ahmed, P. C. Wilson, Rapid cloning of high-affinity human monoclonal antibodies against influenza virus. *Nature* **453**, 667–671 (2008).
26. F. E.-H. Lee, J. L. Halliley, E. E. Walsh, A. P. Moscatiello, B. L. Kmush, A. R. Falsey, T. D. Randall, D. A. Kaminiski, R. K. Miller, I. Sanz, Circulating human antibody-secreting cells during vaccinations and respiratory viral infections are characterized by high specificity and lack of bystander effect. *J. Immunol.* **186**, 5514–5521 (2011).
27. W. Dejnirattisai, W. Wongwiwat, S. Supasa, X. Zhang, X. Dai, A. Rouvinski, A. Jumnainsong, C. Edwards, N. T. H. Quyen, T. Duangchinda, J. M. Grimes, W.-Y. Tsai, C.-Y. Lai, W.-K. Wang, P. Malasit, J. Farrar, C. P. Simmons, Z. H. Zhou, F. A. Rey, J. Mongkolsapaya, G. R. Screaton, A new class of highly potent, broadly neutralizing antibodies isolated from viremic patients infected with dengue virus. *Nat. Immunol.* **16**, 170–177 (2015).
28. W. Dejnirattisai, A. Jumnainsong, N. Onsirisakul, P. Fitton, S. Vasanawathana, W. Limpitikul, C. Puttikhunt, C. Edwards, T. Duangchinda, S. Supasa, K. Chawansuntati, P. Malasit, J. Mongkolsapaya, G. Screaton, Cross-reacting antibodies enhance dengue virus infection in humans. *Science* **328**, 745–748 (2010).
29. A. Rouvinski, P. Guardado-Calvo, G. Barba-Spaeth, S. Duquerroy, M.-C. Vaney, C. M. Kikuti, M. E. Navarro Sanchez, W. Dejnirattisai, W. Wongwiwat, A. Haouz, C. Girard-Blanc, S. Petres, W. E. Shepard, P. Desprès, F. Arenzana-Seisdedos, P. Dussart, J. Mongkolsapaya, G. R. Screaton, F. A. Rey, Recognition determinants of broadly neutralizing human antibodies against dengue viruses. *Nature* **520**, 109–113 (2015).
30. H. Zhao, E. Fernandez, K. A. Dowd, S. D. Speer, D. J. Platt, M. J. Gorman, J. Govero, C. A. Nelson, T. C. Pierson, M. S. Diamond, D. H. Fremont, Structural basis of Zika virus-specific antibody protection. *Cell* **166**, 1016–1027 (2016).
31. M. K. Gentry, E. A. Henchal, J. M. McCown, W. E. Brandt, J. M. Dalrymple, Identification of distinct antigenic determinants on dengue-2 virus using monoclonal antibodies. *Am. J. Trop. Med. Hyg.* **31**, 548–555 (1982).
32. T. Oliphant, G. E. Nybakken, M. Engle, Q. Xu, C. A. Nelson, S. Sukupolvi-Petty, A. Marri, B.-E. Lachmi, U. Olshevsky, D. H. Fremont, T. C. Pierson, M. S. Diamond, Antibody recognition and neutralization determinants on domains I and II of West Nile virus envelope protein. *J. Virol.* **80**, 12149–12159 (2006).
33. L. J. McHeyzer-Williams, P. J. Milpied, S. L. Okitsu, M. G. McHeyzer-Williams, Class-switchedmemory B cells remodel BCRs within secondary germinal centers. *Nat. Immunol.* **16**, 296–305 (2015).
34. G. V. Zuccarino-Catania, S. Sadanand, F. J. Weisel, M. M. Tomayko, H. Meng, S. H. Kleinstein, K. L. Good-Jacobson, M. J. Shlomchik, CD80 and PD-L2 define functionally distinct memory B cell subsets that are independent of antibody isotype. *Nat. Immunol.* **15**, 631–637 (2014).
35. K. A. Pape, J. J. Taylor, R. W. Maul, P. J. Gearhart, M. K. Jenkins, Different B cell populations mediate early and late memory during an endogenous immune response. *Science* **331**, 1203–1207 (2011).
36. T. M. Garcia-Bates, M. T. Cordeiro, E. J. M. Nascimento, A. P. Smith, K. M. Soares de Melo, S. P. McBurney, J. D. Evans, E. T. A. Marques Jr., S. M. Barratt-Boyes, Association between magnitude of the virus-specific plasmablast response and disease severity in dengue patients. *J. Immunol.* **190**, 80–87 (2013).
37. G. Blanchard-Rohner, A. S. Pulickal, C. M. Jol-van der Zijde, M. D. Snape, A. J. Pollard, Appearance of peripheral blood plasma cells and memory B cells in a primary and secondary immune response in humans. *Blood* **114**, 4998–5002 (2009).
38. D. F. Robbiani, L. Bozzacco, J. R. Keeffe, R. Khouri, P. C. Olsen, A. Gazumyan, D. Schaefer-Babajew, S. Avila-Rios, L. Nogueira, R. Patel, S. A. Azzopardi, L. F. K. Uhl, M. Saeed, E. E. Sevilla-Reyes, M. Agudelo, K.-H. Yao, J. Golijanin, H. B. Gristick, Y. E. Lee, A. Hurley, M. Caskey, J. Pai, T. Oliveira, E. A. Wunder Jr., G. Sacramento, N. Nery Jr., C. Orge, F. Costa, M. G. Reis, N. M. Thomas, T. Eisenreich, D. M. Weinberger, A. R. P. de Almeida, A. P. West Jr., C. M. Rice, P. J. Bjorkman, G. Reyes-Teran, A. I. Ko, M. R. MacDonald, M. C. Nussenzweig, Recurrent potent human neutralizing antibodies to Zika virus in Brazil and Mexico. *Cell* **169**, 597–609.e11 (2017).
39. J. H. Kim, I. Skountzou, R. Compans, J. Jacob, Original antigenic sin responses to influenza viruses. *J. Immunol.* **183**, 3294–3301 (2009).
40. S. Fazekas de St. Groth, R. G. Webster, Disquisitions of original antigenic Sin. I. Evidence in man. *J. Exp. Med.* **124**, 331–345 (1966).
41. Y. S. Choi, Y. H. Baek, W. Kang, S. J. Nam, J. Lee, S. You, D.-Y. Chang, J.-C. Youn, Y. K. Choi, E.-C. Shin, Reduced antibody responses to the pandemic (H1N1) 2009 vaccine after recent seasonal influenza vaccination. *Clin. Vaccine Immunol.* **18**, 1519–1523 (2011).
42. C. M. Midgley, M. Bajwa-Joseph, S. Vasanawathana, W. Limpitikul, B. Wills, A. Flanagan, E. Waiyaiya, H. B. Tran, A. E. Cowper, P. Chotiyarnwong, J. M. Grimes, S. Yoksan, P. Malasit, C. P. Simmons, J. Mongkolsapaya, G. R. Screaton, An in-depth analysis of original antigenic sin in dengue virus infection. *J. Virol.* **85**, 410–421 (2011).
43. S. B. Halstead, S. Rojanasuphot, N. Sangkawibha, Original antigenic sin in dengue. *Am. J. Trop. Med. Hyg.* **32**, 154–156 (1983).
44. P. Abbink, R. A. Larocca, R. A. De La Barrera, C. A. Bricault, E. T. Moseley, M. Boyd, M. Kirilova, Z. Li, D. Ng'ang'a, O. Nanayakkara, R. Nityanandam, N. B. Mercado, E. N. Borducchi, A. Agarwal, A. L. Brinkman, C. Cabral, A. Chandrashekar, P. B. Giglio, D. Jetton, J. Jimenez, B. C. Lee, S. Mojta, K. Molloy, M. Shetty, G. H. Neubauer, K. E. Stephenson, J. P. S. Peron, P. M. d. A. Zanotto, J. Misamore, B. Finneyfrock, M. G. Lewis, G. Alter, K. Modjarrad, R. G. Jarman, K. H. Eckels, N. L. Michael, S. J. Thomas, D. H. Barouch, Protective efficacy of multiple vaccine platforms against Zika virus challenge in rhesus monkeys. *Science* **353**, 1129–1132 (2016).
45. K. A. Dowd, S.-Y. Ko, K. M. Morabito, E. S. Yang, R. S. Pelc, C. R. DeMaso, L. R. Castilho, P. Abbink, M. Boyd, R. Nityanandam, D. N. Gordon, J. R. Gallagher, X. Chen, J.-P. Todd, Y. Tsybovsky, A. Harris, Y.-J. S. Huang, S. Higgs, D. L. Vanlandingham, H. Andersen, M. G. Lewis, R. De La Barrera, K. H. Eckels, R. G. Jarman, M. C. Nason, D. H. Barouch, M. Roederer, W.-P. Kong, J. R. Mascola, T. C. Pierson, B. S. Graham, Rapid development of a DNA vaccine for Zika virus. *Science* **354**, 237–240 (2016).
46. R. A. Larocca, P. Abbink, J. P. S. Peron, P. M. d. A. Zanotto, M. J. Iampietro, A. Badamchi-Zadeh, M. Boyd, D. Ng'ang'a, M. Kirilova, R. Nityanandam, N. B. Mercado, Z. Li, E. T. Moseley, C. A. Bricault, E. N. Borducchi, P. B. Giglio, D. Jetton, G. Neubauer, J. P. Nkolola, L. F. Maxfield,

R. A. De La Barrera, R. G. Jarman, K. H. Eckels, N. L. Michael, S. J. Thomas, D. H. Barouch, Vaccine protection against Zika virus from Brazil. *Nature* **536**, 474–478 (2016).
47. E. Kim, G. Erdos, S. Huang, T. Kenniston, L. D. Falo Jr., A. Gambotto, Preventative vaccines for Zika virus outbreak: Preliminary evaluation. *EBioMedicine* **13**, 315–320 (2016).
48. N. Pardi, M. J. Hogan, R. S. Pelc, H. Muramatsu, H. Andersen, C. R. DeMaso, K. A. Dowd, L. L. Sutherland, R. M. Scearce, R. Parks, W. Wagner, A. Granados, J. Greenhouse, M. Walker, E. Willis, J.-S. Yu, C. E. McGee, G. D. Sempowski, B. L. Mui, Y. K. Tam, Y.-J. Huang, D. Vanlandingham, V. M. Holmes, H. Balachandran, S. Sahu, M. Lifton, S. Higgs, S. E. Hensley, T. D. Madden, M. J. Hope, K. Karikó, S. Santra, B. S. Graham, M. G. Lewis, T. C. Pierson, B. F. Haynes, D. Weissman, Zika virus protection by a single low-dose nucleoside-modified mRNA vaccination. *Nature* **543**, 248–251 (2017).
49. J. M. Richner, S. Himansu, K. A. Dowd, S. L. Butler, V. Salazar, J. M. Fox, J. G. Julander, W. W. Tang, S. Shresta, T. C. Pierson, G. Ciaramella, M. S. Diamond, Modified mRNA vaccines protect against Zika virus infection. *Cell* **169**, 176 (2017).
50. I. J. Fuss, M. E. Kanof, P. D. Smith, H. Zola, Isolation of whole mononuclear cells from peripheral blood and cord blood. *Curr. Protoc. Immunol.* **Chapter 7**, Unit7.1 (2009).
51. T. Tiller, E. Meffre, S. Yurasov, M. Tsuiji, M. C. Nussenzweig, H. Wardemann, Efficient generation of monoclonal antibodies from single human B cells by single cell RT-PCR and expression vector cloning. *J. Immunol. Methods* **329**, 112–124 (2008).
52. B. Briney, K. Le, J. Zhu, D. R. Burton, Clonify: Unseeded antibody lineage assignment from next-generation sequencing data. *Sci. Rep.* **6**, 23901 (2016).
53. J. D. Brien, H. M. Lazear, M. S. Diamond, Propagation, quantification, detection, and storage of West Nile virus. *Curr. Protoc. Microbiol.* **31**, 15D.3.1–15D.3.18 (2013).
54. Z. A. Bornholdt, H. L. Turner, C. D. Murin, W. Li, D. Sok, C. A. Souders, A. E. Piper, A. Goff, J. D. Shamblin, S. E. Wollen, T. R. Sprague, M. L. Fusco, K. B. J. Pommert, L. A. Cavacini, H. L. Smith, M. Klempner, K. A. Reimann, E. Krauland, T. U. Gerngross, K. D. Wittrup, E. O. Saphire, D. R. Burton, P. J. Glass, A. B. Ward, L. M. Walker, Isolation of potent neutralizing antibodies from a survivor of the 2014 Ebola virus outbreak. *Science* **351**, 1078–1083 (2016).
55. R. D. Gietz, R. H. Schiestl, High-efficiency yeast transformation using the LiAc/SS carrier DNA/PEG method. *Nat. Protoc.* **2**, 31–34 (2007).

Acknowledgments: We thank C. Williams and S. M. Eagol for assistance with figure preparation. We thank D. Watkins and D. Magnani for supplying viral stocks for these studies and T. Fredeking for assistance in sample identification. We thank D. Fremont and H. Zhao for DIII, WNV, and the E-FL proteins. **Funding:** This work was supported by a grant from the Defense Advanced Research Projects Agency (DARPA) Autonomous Diagnostics to Enable Prevention and Therapeutics: Prophylactic Options to Environmental and Contagious Threats (ADEPT-PROTECT) program (W31P4Q-13-1-0011). **Author contributions:** L.M.W. wrote the manuscript. T.F.R., E.C.G., D.S., and D.R.B. edited the manuscript. T.F.R., E.C.G., B.B., D.S., N.B., A.S., R.N., K.L., and M.E.B. designed and performed experiments and analyzed results. L.M.W., T.F.R., B.B., D.S., and D.R.B. provided intellectual oversight. L.M.W. and T.F.R. performed the statistical analyses. **Competing interests:** L.M.W., M.E.B., and E.C.G. have an equity position in Adimab LLC. The other authors declare that they have no competing interests.

Submitted 17 May 2017
Resubmitted 2 June 2017
Accepted 24 July 2017
Published 18 August 2017
10.1126/sciimmunol.aan6809

Citation: T. F. Rogers, E. C. Goodwin, B. Briney, D. Sok, N. Beutler, A. Strubel, R. Nedellec, K. Le, M. E. Brown, D. R. Burton, L. M. Walker, Zika virus activates de novo and cross-reactive memory B cell responses in dengue-experienced donors. *Sci. Immunol.* **2**, eaan6809 (2017).

Science Immunology

Zika virus activates de novo and cross-reactive memory B cell responses in dengue-experienced donors

Thomas F. Rogers, Eileen C. Goodwin, Bryan Briney, Devin Sok, Nathan Beutler, Alexander Strubel, Rebecca Nedellec, Khoa Le, Michael E. Brown, Dennis R. Burton and Laura M. Walker

Sci. Immunol. **2**, eaan6809.
DOI: 10.1126/sciimmunol.aan6809

For zika virus, experience counts

For the immune system, practice makes perfect. Previous exposure to an infection elicits a stronger, faster memory response. But how does the immune system respond to a similar but not identical infection? Rogers *et al*. tracked the neutralizing antibody response to zika virus infection in individuals with and without previous exposure to the closely related dengue viruses. They found that zika virus infection primed the preexisting dengue virus response, but that this cross-reactive response was poorly neutralizing. In contrast, de novo zika virus responses were potently neutralizing. These data suggest that zika virus vaccines should target epitopes not present in dengue virus subtypes.

Science Immunology (ISSN 2470-9468) is published by the American Association for the Advancement of Science, 1200 New York Avenue NW, Washington, DC 20005. The title *Science Immunology* is a registered trademark of AAAS.